Molecular Therapy
Methods & Clinical Development
Original Article

Detection and quantification of integrated vector copy number by multiplex droplet digital PCR in dual-transduced CAR T cells

Wei Wang,[1] Muhammad Al-Hajj,[1] and Alireza S. Alavi[1]

[1]Autolus Therapeutics, The MediaWorks, 191 Wood Lane, W12 7FP London, UK

The success of chimeric antigen receptor (CAR) T cell therapies in refractory hematologic malignancies has prompted investigation of their efficacy in solid tumors. AUTO6NG is a dual-transduced GD2-targeting CAR that encodes distinct modules designed to enhance T cell activity in relapsed/refractory neuroblastoma. The ability to detect and precisely quantify vector copy number (VCN) for each integrated vector is essential for assessing the effect of each module on T cell tumor infiltration, persistence, and clinical activity. Droplet digital PCR (ddPCR) enables accurate, sensitive, and absolute quantification of specific nucleic acid sequences. Compared to standard detection of two targets, multiplex ddPCR assays allow simultaneous detection of up to four targets by selective modulation of signal amplitude while retaining the ability to quantify the target. We have developed a multiplex assay based on the two-channel system for simultaneous detection and quantification of three targets in AUTO6NG CAR T cells. The assay was highly specific, sensitive, accurate, and reproducible across time and samples. No differences were observed in measuring VCN between standard duplex and multiplex assays. Our results demonstrate that ddPCR is an accurate and cost-effective method for simultaneous detection of multiple targets in genomic DNA derived from engineered CAR T cells.

INTRODUCTION

Adoptive T cell therapy involves the genetic reprogramming of cytotoxic T cells, through the expression of chimeric antigen receptors (CARs) on the cell surface, enabling them to recognize cell surface antigen(s) expressed on malignant cells. CARs are composed of an extracellular domain designed to bind a target with high specificity, without major histocompatibility complex restriction, and intracellular signaling domains that promote T cell activation.[1,2] CAR T cell therapy has been most extensively evaluated in B cell malignancies. Encouraging results have been reported for patients with chronic lymphocytic leukemia and acute lymphoblastic leukemia using CD19-directed CAR T cells.[3–6]

Neuroblastoma is a rare embryonal tumor of the sympathetic nervous system, which occurs almost exclusively in children.[7] Promising cell- and antibody-based therapies targeting a tumor-associated antigen, the disialoganglioside GD2 that is highly expressed in neuroblastoma, have significantly improved overall survival.[8–12]

AUTO6 is an autologous T cell transduced with a gamma-retroviral vector encoding both an anti-GD2 CAR and the RQR8 suicide gene. The ongoing phase I clinical study of GD2-targeted CART for refractory/relapsed neuroblastoma (NCT02761915) shows activity against disseminated disease without inducing on target/off tumor toxicity.[11] To improve the efficacy of AUTO6 in neuroblastoma and other solid tumor indications, we designed AUTO6NG using two retroviral vectors that encode additional cell programming modules to enhance expansion, persistence, and tumor infiltration by counteracting potential immunosuppressive factors within the tumor microenvironment. An assessment of peripheral blood or tumor biopsies for the prevalence of CAR T cells harboring such modules can provide critical information about the mechanisms of clinical activity and resistance.

Analysis of CAR T cell persistence has been traditionally performed by quantitative real-time PCR amplifying integrated viral vector sequences in genomic DNA obtained from biospecimens. More recently, droplet digital PCR (ddPCR) has emerged as a more accurate and precise method for quantification of vector copy number (VCN) as a surrogate for CAR T cell persistence in clinical trials.[13–19] The standard ddPCR assay is a duplex reaction that enables simultaneous detection of viral vector sequences as well as an endogenous sequence to quantify genomic DNA input.[13] The higher order multiplexing ddPCR assay has recently be adapted to allow multiplexed detection of more than two targets in the same droplet by varying the concentrations of different primer-probes using the same fluorophore to modulate the endpoint droplet signal amplitude in the reaction.[20–22]

Herein, we have applied multiplexed ddPCR for the detection and precise quantification of two integrated targets sequences as well as an endogenous target in dual-transduced AUTO6NG CAR T cells.

Received 25 November 2020; accepted 12 July 2023;
https://doi.org/10.1016/j.omtm.2023.07.003.

Correspondence: Wei Wang, Autolus Therapeutics, The MediaWorks, 191 Wood Lane, W12 7FP London, UK.
E-mail: w.wang@autolus.com

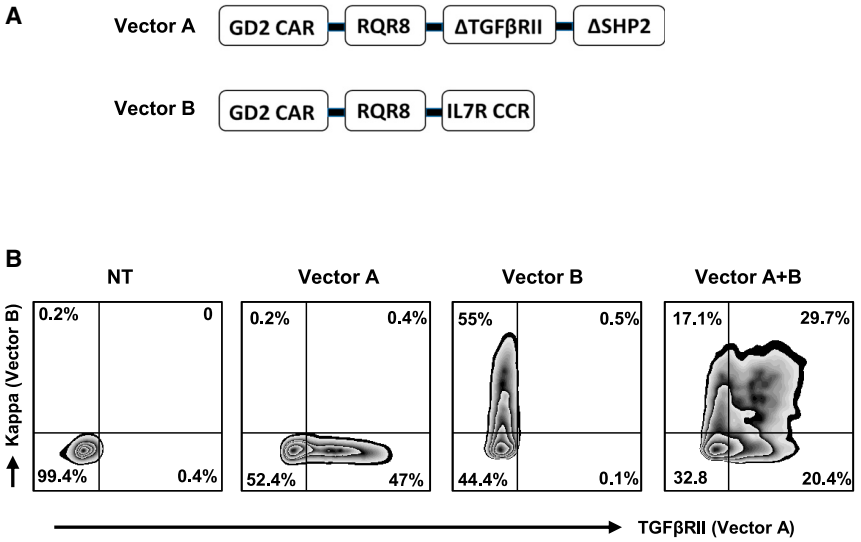

Figure 1. Viral vectors and generation of CAR T cells
(A) Schematic of the AUTO6NG CAR constructs. Vectors A and B consist of the following modules: GD2-targeting receptor (GD2 CAR), RQR8 suicide module, dominant-negative TGFβRII protein (ΔTGFβRII), truncated SHP2 protein (ΔSHP2), and the common γ chain (g-chain) heterodimerized with an IL7 receptor chimeric cytokine receptor (IL7R CCR) module. Sequences from SHP2 and g-chain were selected as targets to detect Vector A and Vector B, respectively. (B) AUTO6NG CAR T cells were transduced with two retroviral vectors to generate dual-transduced AUTO6NG and single-transduced control CAR T cells. Non-transduced (NT) T cells served as a negative control. The transduction efficiency was analyzed by flow cytometry using the CD34 antibody recognizing RQR8 construct that is coexpressed with CAR and the antibodies against TGFβRII and kappa light chain fused to the endodomain of the g-chain for Vector A and Vector B, respectively. The representative flow plots were gated on viable, single CD3+ T cells.

We provide evidence that the multiplex assay is as precise as the standard duplex assay. The assay is linear in a range of 5–100,000 copies per reaction for both vector sequences with no interference observed from peripheral blood genomic DNA ranging from 1.25 to 400 ng per reaction. Our results demonstrate that the multiplex assay is sensitive, precise, robust, and reproducible, highlighting its utility in characterization of integrated sequences in complex CAR T populations.

RESULTS

Generation of CAR T cells

Three types of CAR T cells were generated with the transduction of two retroviral vectors. Vector A single-transduced CAR T cells (Vector A) express a CAR against the GD2 target, a dominant-negative TGFβRII protein (ΔTGFβRII) to block signaling from TGFβ, a truncated SHP2 protein (ΔSHP2) to block PD1 signaling, and a RQR8 suicide receptor as a safety switch to enable control of CAR T cell activity after infusion.[23–26] Vector B single-transduced CAR T cells (Vector B) express the GD2 CAR, the common γ chain (g-chain) heterodimerized with a constitutively signaling IL7 cytokine receptor chimeric cytokine receptor (IL7R CCR) encoding sequence to enhance CAR T cell persistence, and the RQR8 receptor[26–28] (Figure 1A). Activated T cells were transduced with Vector A, Vector B, or both, and the transduction efficiency was analyzed by flow cytometry using the antibodies against RQR8 expressed on both vectors, TGFβRII and kappa light chain fused to the endodomain of the g-chain for Vector A and B, respectively (Figure 1B). Non-transduced (NT) cells served as a negative control. The cell gating strategy was described as live cells > single cells > CD3+ > CD34+ > TGFβRII (anti-TGFβRII) vs. g-chain (anti-Kappa). The cells transduced with Vector A (Vector A) showed 66% transduction efficiency based on CD34 expression with 75% positive staining for TGFβRII and negative staining for g-chain. Vector B single-transduced cells showed 61% transduction efficiency with 67% positive for g-chain and negative for TGFβRII. Dual-transduced AUTO6NG CAR T cells (Vector A + B) showed 70% positive staining for RQR8 with 19% TGFβRII single-positive, 21% g-chain single-positive, and 33% double-positive transduction. These data demonstrate the specificity of single- and dual-transduced CAR T cells as controls in multiplexed ddPCR assays.

Selection of primers and probes for each vector of AUTO6NG CAR T cells

To quantify the abundance of target vector sequences in genomic DNA derived from peripheral blood, we sought to identify unique sequences from Vector A and Vector B for amplification, aiming to maximize specificity, signal amplitude, and similar annealing temperatures. We selected sequences encoding dominant-negative SHP2 (SHP2) from Vector A and sequences encoding the g-chain heterodimerized with IL7R CCR for Vector B (Figure 1A). Sequences for both targets are codon-optimized and do not share homology with endogenous sequences present in the human genome. Three primer-probe pairs were designed for each target in FAM (6-carboxyfluorescein) channel, SHP2 for Vector A, and g-chain for vector B (Table 1). VCN in CAR T clinical trials is commonly expressed as the number of target sequences detected per microgram of genomic DNA. While each PCR reaction is loaded with 100–200 ng of genomic DNA as measured by spectrophotometry, quantification of an endogenous reference target by ddPCR is used to obtain a measure of the number of diploid genomes and, by inference, the precise quantity of gDNA in the PCR reaction. Commercially available primer/probe sequences from human ribonuclease P protein subunit p30 (RPP30) were used for this purpose (Table 1).

A ddPCR one-dimensional (1D) plot showed that SHP2-positive droplets were visible in the FAM channel with all three primer-probe pairs in single- (Vector A) and double-transduced cells (Vector A + B). There was no false positive signal detected in vector B or NT cells using Vector A reagents (Figure S2A). Similarly, g-chain was specifically detected in the FAM channel with all primer-probe pairs in

Table 1. Design of primer-probe sequences for SHP2, g-chain (FAM), and RPP30 (HEX)

	Forward primer (500 nM)	Reverse primer (500 nM)	Probe (250 nM)
SHP2-1	CAATGACGGCAAGTCCAAAG	GTCAGGCTGTCGAATCTCTC	ATGATCCGGTGCCAGGAACTGAAG
SHP2-2	GACCCACATCAAGATCCAGAA	CCGTGGTGTTCCATGTAGTA	CACCGGCGACTACTACGACCTGTA
SHP2-3	CAAAGTGACCCACGTGATGA	GGGTTTCCACCATAGGGTTT	ACGTCGTACTTCAGTTCCTGGCAC
g-chain-1	TGACTACTCCGAGAGACTGTG	ATAAGGGCTGTGCTGGTTG	CCTGGTGTCCGAGATCCCTCCTAA
g-chain-2	CCTGCTGTGCGTGTACTT	GAGAAGTTGCCGTGGTACTC	CTGGAACGGACCATGCCCAGAATC
g-chain-3	GGCAACTTCTCTGCTTGGA	TTAGGAGGGATCTCGGACAC	TGACTACTCCGAGAGACTGTGCCT
RPP30	AGTAACTTGTAAGTGGTAGTGCATAGA	ATGTCAAGAGTAGGAGGACATTTG	TCAGGCAGACTGACACTAGAGTTC

Vector B single- (Vector B) and double-transduced cells and no signal was detected in Vector A or NT cells (Figure S2B). RPP30 signal was detected in the HEX (hexachloro-fluorescein) channel. The VCN quantification for Vector A using SHP2 as the target with three pairs of primer-probe showed no difference in single- or double-transduced cells (Figure S2C). Based on the standard deviation of the replicates, positive signal intensity, and similarities in Tm, SHP2 pair-1 was selected as the target for Vector A. Similarly, all primer-probe pairs of g-chain showed precise and consistent VCN quantification, and g-chain pair-1 was selected as the Vector B target. Altogether, these data confirm that the designed primers conferred adequate specificity.

Establishment of the multiplex assay

The standard duplex assay enables detection of endpoint fluorescence amplitude and quantification of SHP2 and RPP30 or g-chain and RPP30 in the FAM and HEX channels, respectively, within a single reaction. Higher order multiplexing can be achieved by modulating the primer-probe concentrations for each target and deconvoluting the resulting distribution of signal on the 2D scatterplot. This enables detection of multiple targets simultaneously in two discrete optical channels while retaining the ability to quantify each target with precision. The primer-probe concentrations used for each target are listed in Table 2.

To establish the accuracy of the multiplex assay, quantification of VCN using the same gDNA extracted from dual-transduced AUTO6NG cells (Vector A + B) (Figure 1B) by ddPCR standard and multiplex assays was compared. The standard duplex analysis is illustrated by two-dimensional (2D) scatter graphs (Figures 2A and 2B). The thresholds were set up at 5,000 on the Y axis for SHP2 and g-chain (FAM) and at 3,000 on the X axis for RPP30 (HEX) to separate the positive and negative partitions. The black cluster in the lower left marks the dual-negative droplets. For the multiplex assay, both SHP2 and g-chain targets were detected in FAM channel, and RPP30 was detected in HEX channel. However, SHP2 and g-chain had relative concentrations of 200% and 80% of RPP30, respectively, (Table 2) resulting in eight different clusters (Figure 2C). The concentration of each target and thresholds used were the same as the standard duplex assays. We observed no significant difference between the duplex and the multiplex assays in terms of target copy number per reaction or VCN per cell (Figures 2D and 2E), suggesting that one multiplex assay is as accurate as two standard duplex assays.

Determination of linearity, precision, limits of detection, and quantitation

The limit of detection (LoD) is the lowest target copy number in a PCR reaction that can be detected at a specified level of confidence, and the limit of quantification (LoQ) is the lowest copy number in a reaction that can be reliably quantified with an acceptable level of precision and accuracy.[29,30] To establish the sensitivity and accuracy of the multiplex ddPCR system, the linear range, the LoD, and LoQ of the assay were determined.

To determine the linear range of SHP2 and g-chain VCN by multiplex assay, an 11-point dilution series (5–500,000 copies) of Vector A plasmid encoding SHP2 and Vector B plasmid encoding g-chain was prepared in a constant background of 100 ng human gDNA per reaction. No DNA template served as a negative control (Blank). Serial dilutions (10 replicates each) were then analyzed by ddPCR and compared with expected counts (Table S1). The QuantaSoft software failed to report measured values at the highest concentration of 500,000 copies per reaction; therefore, 100,000 copies per reaction was considered the upper LoD and quantitation for the assay. The mean, standard deviation (SD), and the coefficient of variation (CV) were calculated. Both SHP2 and g-chain showed good correlation between expected and measured values with R^2 values of 0.9985 and 0.9994, respectively, establishing 5–100,000 copies as the linear range of the assay (Figure 3A). The SHP2 and g-chain sequences in the reaction had no impact on the detected RPP30 copy number (Table S2).

We next calculated the lower LoD as the mean of Blank + (3.3 x SD of the lowest concentration where CV is less than 40%). The LoQ was calculated as the mean of Blank + (10 x SD of the lowest concentration where CV is less than 40%) (29). The LoD and LoQ for SHP2 target were calculated as 10 copies and 30 copies per reaction, respectively (Table S1). Similarly, the LoD and LoQ for g-chain target were calculated as 7 copies and 20 copies per reaction, respectively (Table S1).

Finally, we evaluated the effect of different quantities of gDNA extracted from peripheral blood on VCN for each target. A 12-point

Table 2. Primer-probe concentrations use for the duplex and multiplex assays

	Forward primer	Reverse primer	Probe
SHP2	1,000 nM	1,000 nM	500 nM
g-chain	400 nM	400 nM	200 nM
RPP30	500 nM	500 nM	250 nM

serial dilution of gDNA (10 replicates each) ranging from 400 ng to 0.01 ng per reaction was evaluated in a constant background of Vector A and Vector B sequences (Table S2). Expected and measured RPP30 copy numbers are strongly correlated with an R^2 value of 0.9896 (Figure 3B). Importantly, we observed no significant interference from 0.25–400 ng purified peripheral blood gDNA on SHP2 and g-chain VCN in this assay.

Assessment of variation in VCN quantification across time

To evaluate variation in quantifying VCN across time in the multiplex assay, we evaluated the VCN from three aliquots of the same batch of AUTO6NG CAR T cells cryopreserved and thawed at different time points (R1, week 0; R2, week 2; and R3, week 4). The VCN was established by multiplex assay in parallel with the standard duplex assay. We observed no difference in SHP2 or g-chain VCN between these two assays or across time points over a 2-week period (Figure 4). These results suggest that multiplexed ddPCR can be used to determine the VCN for each vector of dual-transduced AUTO6NG CAR T cells accurately and consistently across time.

DISCUSSION

ddPCR has several advantages compared to standard real-time PCR, including higher sensitivity and accuracy.[13] It provides absolute quantification without external calibration curves, which reduces variability between assays and difficulty in measuring targets from samples with low numbers of cells. Standard duplex ddPCR is increasingly used for precise determination of persistence in CAR T clinical trials.[14–19] Here, we have extended the ddPCR assay to detect two integrated viral sequences along with an endogenous sequence in the same droplet. To our knowledge, the present manuscript is the first study demonstrating multiplexed assessment of VCN in dual-transduced CAR T cells. Our results show that the multiplex assay is as sensitive, precise, and robust as the corresponding duplex analysis. However, the multiplexed assay described in this study does not provide single-cell-level information, but rather it quantifies proportional representation of each sequence at the population level including all single- and dual-transduced cells as well all NT nucleated cells from which gDNA is derived.

Accurate estimation of VCN in transduced cells is essential for monitoring CAR T cell expansion and long-term persistence after infusion in the treated patients.[31] As engineered CAR T cells gain additional functionality to overcome immune challenges in the solid tumor setting, precise characterization of complex populations derived from biospecimens can lead to a better understanding of the interplay between the tumor microenvironment and CAR T cell infiltration, expansion, and persistence. One powerful application of the multiplexed assay is to evaluate the relative abundance of specific modules in various compartments of a tumor biopsy to better understand immunosuppressive mechanisms and to guide the design of more effective vectors.

The multiplex assay provides a precise and reliable for rapid quantitation of the relative abundance of specific viral sequences in engineered T cells. It minimizes the cost for analysis and enables more information compared to the standard assay, particularly for the samples with limited input. Furthermore, the assay can be rapidly adapted to detect new target genomic DNA sequences, or transcripts when combined with a reverse transcription step. However, the reproducibility of the assay, such as the variation in measuring VCN across analysts, laboratories, and instruments is required for further evaluation.[21,22]

In this study, we describe a triplex ddPCR assay that enables quantification of two target sequences through signal deconvolution. However, the platform is amenable to higher order multiplexing by addition of a second target to the HEX channel or through further refinements in reagent concentrations to modulate signal amplitude and introduction of automated signal deconvolution algorithms. Overall, multiplexed ddPCR offers a robust and cost-effective approach to rapid analysis of complex CAR T cell populations in clinical samples.

MATERIALS AND METHODS

AUTO6NG CAR T cell production

The AUTO6NG CAR T cell production method was prepared as described previously.[11] Briefly, peripheral blood mononuclear cells from healthy donors were activated with anti-CD3 (clone OKT3, 100 ng/mL, Miltenyi Biotec, Bergisch Gladbach, Germany) and anti-CD28 monoclonal antibodies (clone 15E8, 100 ng/mL, Miltenyi Biotec) and human recombinant human IL-7/IL-15 cytokines (10 ng/mL, PeproTech, London, UK) to induce T cell proliferation. The cells were then transduced with two retroviral vectors: Vector A encoded a GD2 CAR and SHP2/TGFβRII dominant-negative modules, and Vector B encoded a GD2 CAR and IL7R CCR module. The cells were expanded for 5 days after initial transduction and were assessed by flow cytometry for transduction efficiency and by ddPCR analysis for VCN.

DNA isolation and quantification

Genomic DNA (gDNA) was extracted from AUTO6NG CAR T cells and NT control cells using a Qiagen QIAamp DSP DNA Blood Mini Kit (Qiagen, Hilden, Germany) according to the manufacturer's instructions. The purity and concentration of the isolated dnaA260/A280 ratio was measured using a Nanodrop One spectrophotometer (Thermo Fisher Scientific, Waltham, MA).

ddPCR duplex and multiplex assays

ddPCR duplex and multiplex assays were performed using a Bio-Rad Auto DG QX200 ddPCR system (Bio-Rad Laboratories, Hercules,

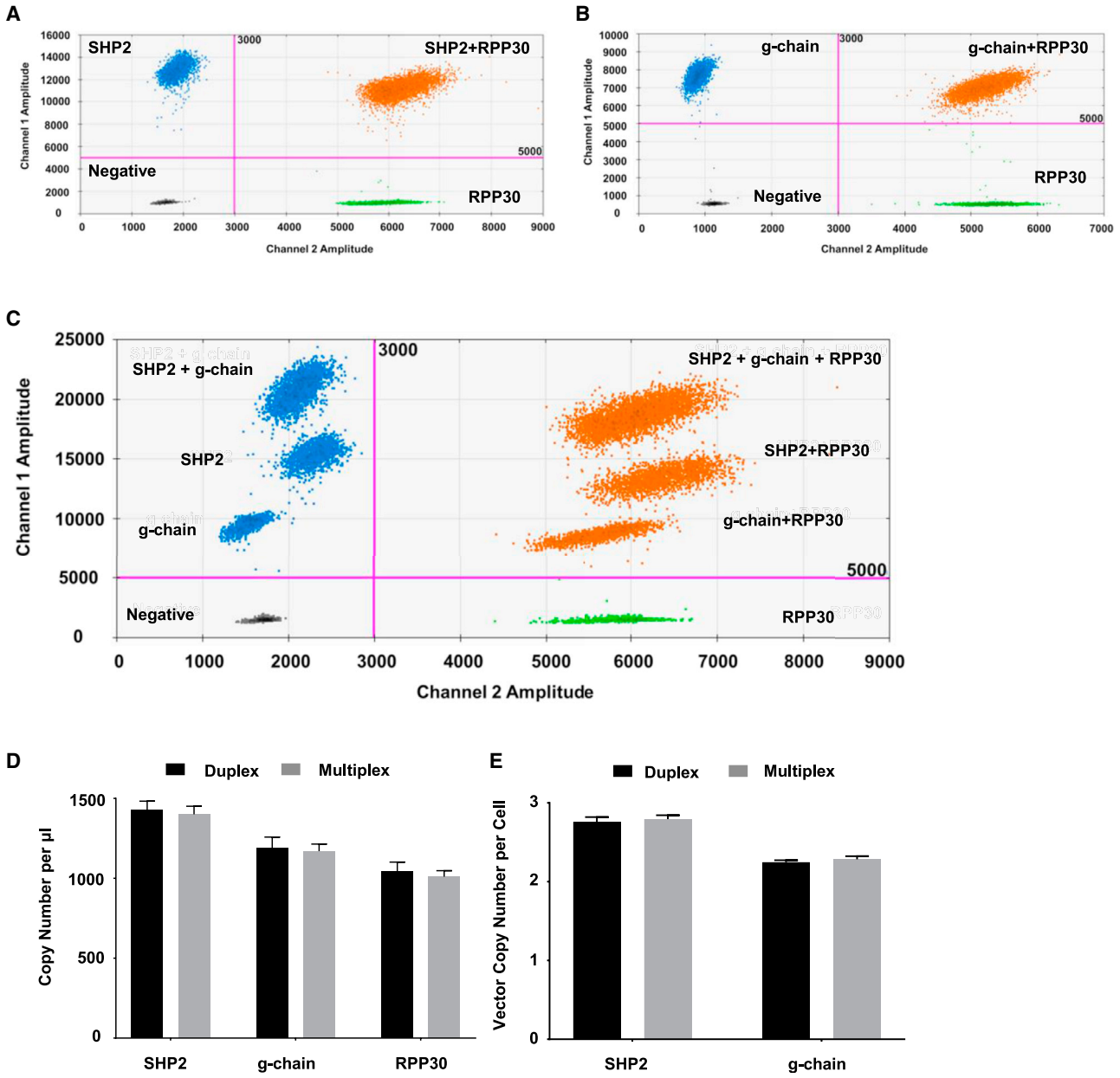

Figure 2. Comparison of SHP2 and g-chain VCN quantification by duplex and multiplex assays

ddPCR VCN analysis using the same gDNA extracted from AUTO6NG dual-transduced cells by standard and multiplex assays. Representative 2D scatterplots showing the detection of (A) SHP2/RPP30 and (B) g-chain/RPP30 positive droplets by a standard duplex ddPCR assay: double-negative (black), SHP2/g-chain single-positive (FAM: blue), RPP30 single-positive (HEX: green), and double positives (orange). (C) Representative 2D scatterplot showing SHP2 and g-chain positive droplets (FAM) and RPP30 (HEX) droplets in a multiplexed ddPCR reaction resulting in eight clusters. (D) Comparison of SHP2, g-chain, and RPP30 sequence copy numbers between the duplex and multiplex ddPCR assays. (E) Comparison of SHP2 and g-chain VCN assessments between duplex and multiplexed assays normalized to RPP30 (copies per cell). Bars indicate mean values with SDs (n = 4).

CA) according to the manufacturer's instructions. All designed pairs of primer-probe for targets were cross-checked with binding sites against the human genome to ensure target specificity (Primer-BLAST, NCBI) and purchased from IDT (Integrated DNA Technologies, Coralville, USA.). The details for primer-probe pairs are provided in Table 1. A temperature gradient analysis determined 59°C to be the optimal annealing temperature in the duplex and multiplex assays with SHP2 and g-chain vector constructs (Figure S1). ddPCR was performed using 1X ddPCR Supermix for probes (no dUTP, Bio-Rad Laboratories) and 20 units of HindIII restriction enzyme

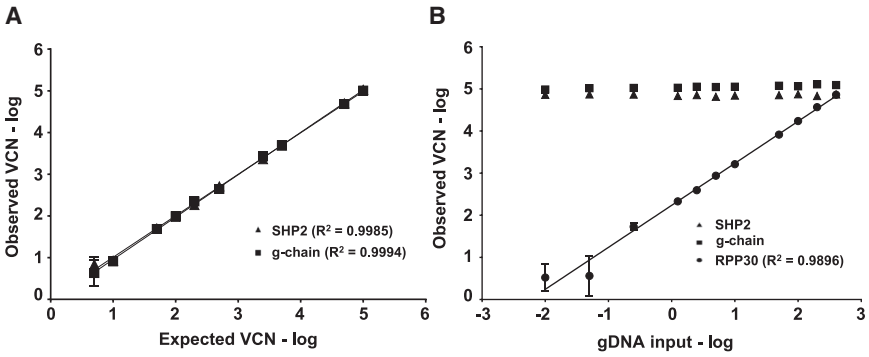

Figure 3. Determination of linearity, precision, and gDNA interference in the multiplexed ddPCR assay

(A) Detection of SHP2 and g-chain in a constant background of 100 ng gDNA (10-point serial dilutions from 100,000 to 5 copies, 10 replicates each). The expected and observed VCNs are indicated on the X and Y axes, respectively (Log10). Both SHP2 (R^2 = 0.9985) and g-chain (R^2 = 0.9994) show a high correlation between observed and expected values. (B) RPP30 assay linearity and interference with SHP2 and g-chain VCN assessment. RPP30 copy number was assessed using gDNA input ranging from 0.01 to 400 ng in a background of 71,614 and 112,307 copies of Vector A and Vector B per reaction, respectively.

(New England BioLab, Hitchin, UK) in a final 22 μL per reaction with 100 ng of gDNA extracted from the cells. The concentrations of primer-probe were used as indicated. Following droplet generation, between 11,000 and 15,000 on average, the droplets were amplified using a C1000 Touch thermocycler (Bio-Rad Laboratories) with a 105°C heated lid. The thermal cycling program included the enzyme activation at 95°C for 10 min, 40 cycles of denaturing at 94°C for 30 s, and annealing at 59°C for 1 min at a ramp rate of 2°C/s, followed by enzyme deactivation at 98°C for 1 min. The droplets were held at 4°C prior to analysis. No template control reactions were performed using nuclease-free water. The plates containing the droplets were read with QX200 droplet reader (Bio-Rad Laboratories) using a two-channel setting to detect FAM and HEX. The positive droplets containing amplification targets were discriminated from negative droplets without amplification products by applying a fluorescence amplitude threshold. The threshold was set manually as indicated in the middle between the clusters using the 1D or 2D amplitude chart. The concentration of target amplicon per unit volume and estimation of VCN of target gene normalized to the reference gene (RPP30) were determined by QuantaSoft software version 1.7.4.0917 (Bio-Rad Laboratories, Hercules, CA). All the assays worked well according to the minimal information for publication of quantitative digital PCR experiments guidelines.[21,22]

Flow cytometry analysis

The AUTO6NG CAR T cells were analyzed by flow cytometry to assess the transduction efficiency using fluorochrome-labelled antibodies including BUV395 anti-CD3 (clone UCHT1, 1:100 dilution, BD Biosciences, San Jose, CA), APC anti-CD34 (clone # QBEnd10, 1:50 dilution, R&D Systems, Abingdon, UK), FITC anti-TGFβRII (clone # 25508, 1:100 dilution, R&D Systems), PE anti-Kappa for g-chain (clone A8B5, 1:100 dilution, Thermo Fisher Scientific, Waltham, MA), and viability dye FVS780 (1:1,000 dilution, BD Biosciences). Samples were stained and acquired with BD Fortessa flow cytometer (BD Biosciences, San Jose, CA). Data were analyzed with FlowJo software (BD Biosciences, San Jose, CA).

Statistical analysis

GraphPad Prism version 7 software (GraphPad Software, La Jolla, CA) was used for statistical analysis. Data are presented as mean with SD. Two-way ANOVA analysis was used for multiple group comparison. Two-tailed Pearson statistics with a confidence interval of 95% were used to determine correlation coefficients. Probability values ($p < 0.05$) were considered statistically significant.

DATA AND CODE AVAILABILITY

We confirm that the data supporting the findings of the work are available within the article and the supplemental information.

SUPPLEMENTAL INFORMATION

Supplemental information can be found online at https://doi.org/10.1016/j.omtm.2023.07.003.

ACKNOWLEDGMENTS

We would like to thank James Sillibourne for providing CAR vectors and control plasmids and Rebecca Moore for production of single- and dual-transduced CAR T cells.

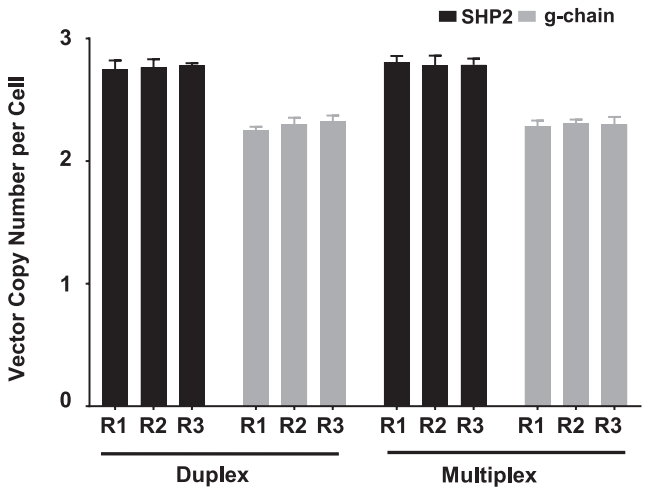

Figure 4. Assessment of short-term stability

Comparison of SHP2 and g-chain VCN assessment by duplex and multiplex ddPCR assays using cryopreserved CAR T cells across three time points spaced 2 weeks apart (R1, week 0; R2, week 2; and R3, week 4). The quantitation was established on VCN per cell. Bars indicate mean values with SDs (n = 3).

AUTHOR CONTRIBUTIONS

W.W., M.A.-H., and A.S.A. conceived of the presented idea. W.W. designed and performed the experiments. A.S.A and M.A.-H. supervised the work and verified the analytical methods. W.W. and A.S.A. wrote the manuscript with support from M.A.-H.

DECLARATION OF INTERESTS

The authors declare no potential conflicts of interest.

REFERENCES

1. Boyiadzis, M.M., Dhodapkar, M.V., Brentjens, R.J., Kochenderfer, J.N., Neelapu, S.S., Maus, M.V., Porter, D.L., Maloney, D.G., Grupp, S.A., Mackall, C.L., et al. (2018). Chimeric antigen receptor (CAR) T therapies for the treatment of hematologic malignancies: clinical perspective and significance. J. Immunother. Cancer *6*, 137. https://doi.org/10.1186/s40425-018-0460-5.
2. Salter, A.I., Pont, M.J., and Riddell, S.R. (2018). Chimeric antigen receptor-modified T cells: CD19 and the road beyond. Blood *131*, 2621–2629. https://doi.org/10.1182/blood-2018-01-785840.
3. Raje, N., Berdeja, J., Lin, Y., Siegel, D., Jagannath, S., Madduri, D., Liedtke, M., Rosenblatt, J., Maus, M.V., Turka, A., et al. (2019). Anti-BCMA CAR T-cell therapy bb2121 in relapsed or refractory multiple myeloma. N. Engl. J. Med. *380*, 1726–1737. https://doi.org/10.1056/nejmoa1817226.
4. Park, J.H., Rivière, I., Gonen, M., Wang, X., Sénéchal, B., Curran, K.J., Sauter, C., Wang, Y., Santomasso, B., Mead, E., et al. (2018). Long-term follow-up of CD19 CAR therapy in acute lymphoblastic leukemia. N. Engl. J. Med. *378*, 449–459. https://doi.org/10.1056/nejmoa1709919.
5. Maude, S.L., Laetsch, T.W., Buechner, J., Rives, S., Boyer, M., Bittencourt, H., Bader, P., Verneris, M.R., Stefanski, H.E., Myers, G.D., et al. (2018). Tisagenlecleucel in children and young adults with B-Cell lymphoblastic leukemia. N. Engl. J. Med. *378*, 439–448. https://doi.org/10.1056/nejmoa1709866.
6. Fry, T.J., Shah, N.N., Orentas, R.J., Stetler-Stevenson, M., Yuan, C.M., Ramakrishna, S., Wolters, P., Martin, S., Delbrook, C., Yates, B., et al. (2018). CD22-targeted CAR T cells induce remission in B-ALL that is naive or resistant to CD19-targeted CAR immunotherapy. Nat. Med. *24*, 20–28. https://doi.org/10.1038/nm.4441.
7. Smith, M.A., Altekruse, S.F., Adamson, P.C., Reaman, G.H., and Seibel, N.L. (2014). Declining childhood and adolescent cancer mortality. Cancer *120*, 2497–2506. https://doi.org/10.1002/cncr.28748.
8. Mujoo, K., Cheresh, D.A., Yang, H.M., and Reisfeld, R.A. (1987). Disialoganglioside GD2 on human neuroblastoma cells: target antigen for monoclonal antibody-mediated cytolysis and suppression of tumor growth. Cancer Res. *47*, 1098–1104.
9. Yu, A.L., Gilman, A.L., Ozkaynak, M.F., London, W.B., Kreissman, S.G., Chen, H.X., Smith, M., Anderson, B., Villablanca, J.G., Matthay, K.K., et al. (2010). Anti-GD2 antibody with GM-CSF, interleukin-2, and isotretinoin for neuroblastoma. N. Engl. J. Med. *363*, 1324–1334. https://doi.org/10.1056/nejmoa0911123.
10. Richards, R.M., Sotillo, E., and Majzner, R.G. (2018). CAR T Cell Therapy for Neuroblastoma. Front. Immunol. *9*, 2380. https://doi.org/10.3389/fimmu.2018.02380.
11. Straathof, K., Flutter, B., Wallace, R., Thomas, S., Cheung, G., Collura, A., Gileadi, T., Barton, J., Wright, G., Inglott, S., et al. (2018). A Cancer Research UK Phase I Trial of Anti-GD2 Chimeric Antigen Receptor (CAR) Transduced T-Cells (1RG-CART) in Patients With Relapsed or Refractory Neuroblastoma. Cancer Res. *78* (13 Suppl), CT145. https://doi.org/10.1158/1538-7445.AM2018-CT145.
12. Long, A.H., Haso, W.M., Shern, J.F., Wanhainen, K.M., Murgai, M., Ingaramo, M., Smith, J.P., Walker, A.J., Kohler, M.E., Venkateshwara, V.R., et al. (2015). 4-1BB costimulation ameliorates T cell exhaustion induced by tonic signaling of chimeric antigen receptors. Nat. Med. *21*, 581–590. https://doi.org/10.1038/nm.3838.
13. Pinheiro, L.B., Coleman, V.A., Hindson, C.M., Herrmann, J., Hindson, B.J., Bhat, S., and Emslie, K.R. (2012). Evaluation of a droplet digital polymerase chain reaction format for DNA copy number quantification. Anal. Chem. *84*, 1003–1011. https://doi.org/10.1021/ac202578x.
14. Lu, A., Liu, H., Shi, R., Cai, Y., Ma, J., Shao, L., Rong, V., Gkitsas, N., Lei, H., Highfill, S.L., et al. (2020). Application of droplet digital PCR for the detection of vector copy number in clinical CAR/TCR T cell products. J. Transl. Med. *18*, 191. https://doi.org/10.1186/s12967-020-02358-0.
15. Fehse, B., Badbaran, A., Berger, C., Sonntag, T., Riecken, K., Geffken, M., Kröger, N., and Ayuk, F.A. (2020). Digital PCR Assays for Precise Quantification of CD19-CAR-T Cells after Treatment with Axicabtagene Ciloleucel. Mol. Ther. Methods Clin. Dev. *16*, 172–178. https://doi.org/10.1016/j.omtm.2019.12.018.
16. Pabst, T., Joncourt, R., Shumilov, E., Heini, A., Wiedemann, G., Legros, M., Seipel, K., Schild, C., Jalowiec, K., Mansouri Taleghani, B., et al. (2020). Analysis of IL-6 serum levels and CAR T cell-specific digital PCR in the context of cytokine release syndrome. Exp. Hematol. *88*, 7–14.e3. https://doi.org/10.1016/j.exphem.2020.07.003.
17. Lock, M., Alvira, M.R., Chen, S.J., and Wilson, J.M. (2014). Absolute determination of single-stranded and self-complementary adeno-associated viral vector genome titers by droplet digital PCR. Hum. Gene Ther. Methods *25*, 115–125. https://doi.org/10.1089/hgtb.2013.131.
18. Lin, H.T., Okumura, T., Yatsuda, Y., Ito, S., Nakauchi, H., and Otsu, M. (2016). Application of droplet digital PCR for estimating vector copy number states in stem cell gene therapy. Hum. Gene Ther. Methods *27*, 197–208. https://doi.org/10.1089/hgtb.2016.059.
19. Igarashi, Y., Uchiyama, T., Minegishi, T., Takahashi, S., Watanabe, N., Kawai, T., Yamada, M., Ariga, T., and Onodera, M. (2017). Single cell-based vector tracing in patients with ADA-SCID treated with stem cell gene therapy. Mol. Ther. Methods Clin. Dev. *6*, 8–16. https://doi.org/10.1016/j.omtm.2017.05.005.
20. Whale, A.S., Huggett, J.F., and Tzonev, S. (2016). Fundamentals of multiplexing with digital PCR. Biomol. Detect. Quantif. *10*, 15–23. https://doi.org/10.1016/j.bdq.2016.05.002.
21. Huggett, J.F., Foy, C.A., Benes, V., Emslie, K., Garson, J.A., Haynes, R., Hellemans, J., Kubista, M., Mueller, R.D., Nolan, T., et al. (2013). The Digital MIQE Guidelines: Minimum Information for Publication of Quantitative Digital PCR Experiments. Clin. Chem. *59*, 892–902. https://doi.org/10.1373/clinchem.2013.206375.
22. dMIQE Group, and Huggett, J.F. (2020). The Digital MIQE Guidelines Update: Minimum Information for Publication of Quantitative Digital PCR Experiments for 2020. Clin. Chem. *66*, 1012–1029. https://doi.org/10.1093/clinchem/hvaa125.
23. Taylor, J., Bulek, A., Gannon, I., Robson, M., Kokalaki, E., Grothier, T., McKenzie, C., El-Kholy, M., Stavrou, M., Traynor-White, C., et al. (2023). Exploration of T cell immune responses by expression of a dominant-negative SHP1 and SHP2. Front. Immunol. *14*, 1119350. https://doi.org/10.3389/fimmu.2023.1119350.
24. Vang, T., Miletic, A.V., Arimura, Y., Tautz, L., Rickert, R.C., and Mustelin, T. (2008). Protein tyrosine phosphatases in autoimmunity. Annu. Rev. Immunol. *26*, 29–55. https://doi.org/10.1146/annurev.immunol.26.021607.090418.
25. Zhang, L., Yu, Z., Muranski, P., Palmer, D.C., Restifo, N.P., Rosenberg, S.A., and Morgan, R.A. (2013). Inhibition of TGF-b signaling in genetically engineered tumor antigen-reactive T cells significantly enhances tumor treatment efficacy. Gene Ther. *20*, 575–580. https://doi.org/10.1038/gt.2012.75.
26. Philip, B., Kokalaki, E., Mekkaoui, L., Thomas, S., Straathof, K., Flutter, B., Marin, V., Marafioti, T., Chakraverty, R., Linch, D., et al. (2014). A highly compact epitope-based marker/suicide gene for easier and safer T-cell therapy. Blood *124*, 1277–1287. https://doi.org/10.1182/blood-2014-01-545020.
27. Cieri, N., Camisa, B., Cocchiarella, F., Forcato, M., Oliveira, G., Provasi, E., Bondanza, A., Bordignon, C., Peccatori, J., Ciceri, F., et al. (2013). IL-7 and IL-15 instruct the generation of human memory stem T cells from naive precursors. Blood *121*, 573–584. https://doi.org/10.1182/blood-2012-05-431718.
28. Matteo, R., Cannon, I., Robson, M., Srivastava, S., Kokalaki, E., Grothier, T., Nannini, F., Allen, C., Bai, Y.V., Sillibourne, J., et al. (2023). Enhancing CAR T cell therapy using Fab-Based Constitutively Heterodimeric Cytokine Receptors. Cancer Immun. https://doi.org/10.1158/2326-6066.cir-22-0640.

29. Topic, E., Nikolac, N., Panteghini, M., Theodorsson, E., Salvagno, G.L., Miler, M., Simundic, A.M., Infusino, I., Nordin, G., and Westgard, S. (2015). How to assess the quality of your analytical method? Clin. Chem. Lab. Med. *53*, 1707–1718. https://doi.org/10.1515/cclm-2015-0869.

30. Holst-Jensen, A., Rønning, S.B., Løvseth, A., and Berdal, K.G. (2003). PCR technology for screening and quantification of genetically modified organisms (GMOs). Anal. Bioanal. Chem. *375*, 985–993. https://doi.org/10.1007/s00216-003-1767-7.

31. Chang, A.H., and Sadelain, M. (2007). The genetic engineering of hematopoietic stem cells: the rise of lentiviral vectors, the conundrum of the ltr, and the promise of lineage-restricted vectors. Mol. Ther. *15*, 445–456. https://doi.org/10.1038/sj.mt.6300060.